Deep-Penetrating Conical Cracks in Brittle Layers from Hydraulic Cyclic Contact

Yu Zhang,* Jun-Kwang Song,† Brian R. Lawn

Materials Science and Engineering Laboratory, National Institute of Standards and Technology, Gaithersburg, Maryland 20899

Received 13 August 2004; accepted 8 September 2004
Published online 25 January 2005 in Wiley InterScience (www.interscience.wiley.com). DOI: 10.1002/jbm.b.30195

Abstract: A study is made of fracture from cyclic loading of WC spheres on the top surfaces of thick (1 mm) brittle layers on polymeric substrates, as representative of repetitive occlusal contact on dental crown structures. The advantage of glass layers is that internal cracks can be followed *in situ* during the entire cyclic loading process. The glass surfaces are first given a surface-abrasion treatment to control the flaw state, such that the strengths match those of dental porcelains. Cyclic contact tests are carried out at prescribed maximum loads and frequencies, in water. In addition to conventional cone cracks that form outside the contact circle, additional, inner cone cracks form within the contact in the water environment. These inner cones are observed only in cyclic loading in water and are accelerated at higher frequencies, indicating a strong mechanical driving force. They tend to initiate after the outer cones, but subsequently catch up and penetrate much more rapidly and deeply, ultimately intersecting the underlying coating/substrate interface. Comparative tests on glass/polymer bilayers versus monolithic glass, in cyclic versus static loading, in water versus air environment, on abraded versus etched surfaces, and with glass instead of WC indenters, confirm the existence of a dominant mechanical element in the inner-cone crack evolution. It is suggested that the source of the mechanical driving force is hydraulic pressure from intrusion and entrapment of liquid in surface fissures at the closing contact interface. This new type of cone cracking may limit dental crown veneer lifetimes under occlusal fatigue conditions, especially in thicker layers, where competing modes—such as undersurface radial cracks—are suppressed. © 2005 Wiley Periodicals, Inc.* J Biomed Mater Res Part B: Appl Biomater 73B: 186–193, 2005

Keywords: biomechanical ceramics; cone cracks; contact damage; cyclic fatigue; fracture modes; hydraulic fracture; glass

INTRODUCTION

Ceramic-based layer systems are used in many engineering and biomechanical applications. Important examples are all-ceramic crowns (replacing enamel) on tooth dentin[1–3] and ceramic acetabular liners in total hip replacements.[4,5] The ceramic layers afford mechanical protection to compliant/soft support underlayers. However, ceramics are subject to life-time-threatening cracking from concentrated contact stresses, especially in sustained and cyclic loading. There is a need to understand how different modes of fracture and deformation compete under such extenuating conditions.

Several damage modes induced by curved indenters in ceramic layers on compliant substrates have been identified and analyzed.[1,2,6–10] These can be divided into two categories: top-surface damage from near-contact stresses, and bottom-surface damage from flexural stresses. Generally, top-surface modes dominate when the coating thickness d is large and sphere radius r is small, especially in sharp-particle contacts; conversely, bottom-surface modes dominate when d is small and r is large. One of the most deleterious fracture modes is radial cracking, usually at the bottom surface, but also, especially in softer ceramics, from quasiplastic deformation zones at the top surface. Such radial cracks are oriented normal to the plate surface and are therefore susceptible to any superposed tensile stresses generated during biomechanical function.

Another top-surface fracture mode associated with curved indenters is that of classical Hertzian cone cracking.[11–16] In single-cycle loading, ring cracks form just outside the contact. Because they tend to remain shallow and at a low angle

Information of product names and suppliers in this article does not imply endorsement by NIST

*On leave from: New York University College of Dentistry, 345 East 24th Street, New York, NY 10010

†On leave from: Machine & Material Center, Korea Testing Laboratory, Guro-Dong, Guro-Gu, Seoul 152-848, Korea

Correspondence to: Brian R. Lawn (e-mail: brian.lawn@nist.gov)

Contract grant sponsor: National Institute of Dental and Craniofacial Research; contract grant number: PO1 DE10976

Contract grant sponsor: Korea Institute S & T Evaluation and Planning (KISTEP) through the National Research Laboratory

© 2005 Wiley Periodicals, Inc. *This article is a US Government work and, as such, is in the public domain in the United States of America.

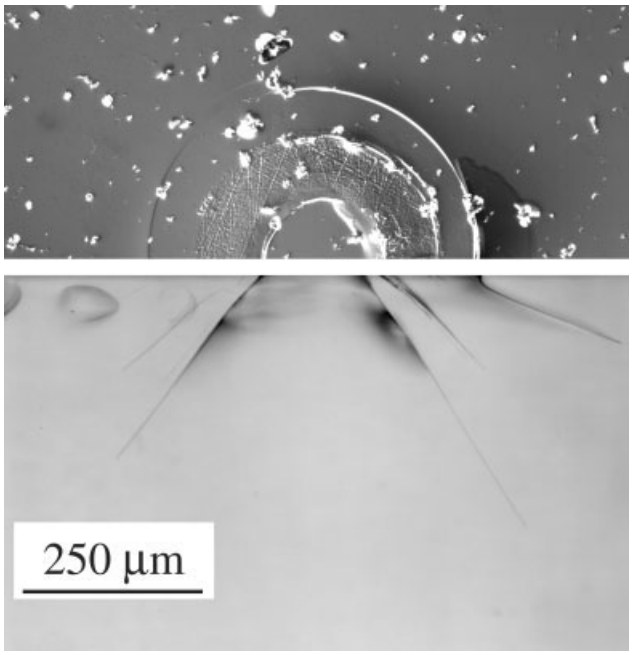

Figure 1. Half-surface and side-section views of Hertzian indentation sites in soda-lime glass, showing outer and inner-cone cracks formed during cycling (WC sphere radius $r = 3.18$ mm, load $P_{max} = 140$ N, cycles $n = 10^4$) in water. Note annular fretting zone. Reproduced from Kim et al.[17]

relative to the specimen surface, even after prolonged loading, these *outer* cracks are not usually considered to be so deleterious to structural integrity. However, there is a second, less well-studied but potentially more dangerous, *inner*-cone crack that forms predominantly in cyclic loading in water.[17] In highly brittle materials like glasses or fine-grain polycrystalline ceramics, inner-cone cracks can appear before radial cracks. An example, reproduced from Kim et al.,[17] is shown in Figure 1. The inner cracks form much steeper angles to the surface and ultimately propagate much deeper into the layer. They start from close to the inner radius of an annular fretting zone, where frictional slippage occurs between the cycling indenter and specimen.[18] Although they do not appear to severely degrade the strength of monolithic ceramics,[17] inner-cone cracks can lead to failure in bilayers by penetrating the brittle coating layer and causing delamination.[19]

This study investigates the mechanics of inner-cone crack evolution in brittle bilayers. The experiments are on model bilayer systems consisting of glass plates bonded to polycarbonate substrates, loaded at the top surfaces with hard spheres in cyclic loading, in water.[20] Glass may be considered to be representative of brittle ceramics (e.g., porcelain), polycarbonate representative of a compliant support (dentin), and water of an oral environment. The glass is sufficiently thick (1 mm) that top-surface cracks dominate over potential competitors (e.g., undersurface radial cracks), but not so much that flexural stresses are eliminated. Cone crack evolution in the glass layers is followed *in situ* during the cycling. Tests on thick monolithic glass plates are used as a baseline comparison. Although the inner-cone cracks are relatively sluggish in their initial growth, they overtake their outer counterparts and penetrate deep into the brittle subsurface after sustained cycling, ultimately causing delamination failure in bilayer specimens. Additional comparative tests are carried out in cyclic versus static loading, in water versus air environment, on abraded versus acid-etched surfaces, and with glass instead of WC indenters. These tests confirm the existence of a dominant mechanical element in the inner-cone crack evolution. Potential sources of this mechanical element are considered, including hydraulic pressure from intrusion and subsequent entrapment of water in surface fissures.[21] The results demonstrate how the various failure modes may dominate under different conditions of testing, so that a primary mode in single-cycle loading may become secondary in cyclic loading.

EXPERIMENTAL METHOD

Soda-lime glass plates measuring 35×25 mm and of thickness $d = 1$ mm were used as a model brittle-layer material.[20] The plates were bonded to polycarbonate substrates 12.5 mm thick with a thin layer (10 μm) of epoxy resin. Bottom surfaces were pre-etched with 4% HF for 5 min to remove surface-handling flaws, and thus to minimize undersurface radial cracks in the subsequent tests.[9] The top surfaces were abraded with 600-grit SiC paper to introduce controlled flaws, to ensure top-surface cracking and to reduce the glass strength to be near that of porcelain.[20,22] Soda-lime glass plates $35 \times 25 \times 5.8$ mm were used as monolithic brittle specimens for comparative testing.

Contact fatigue tests were carried out by loading the specimen top surface with a WC sphere of radius $r = 1.58$ mm, between prescribed maximum and minimum loads $P_{max} = 120$ N and $P_{min} = 2$ N, for n cycles at frequency $f = 1$ Hz. (The minimum load was imposed to prevent the sphere "wandering" over the specimen surface.) Figure 2 defines the cone crack configurations: c is cone crack depth and α is cone angle. For most tests, a drop of water was placed in the contact zone and refreshed throughout the duration of the experiment. Some comparative tests were carried out at frequency $f = 10$ Hz and in static loading for prescribed test durations t at the same P_{max} (with rapid load/unload ramps). Others were conducted in air instead of water, on acid-etched instead of abraded top surfaces, with glass instead of WC indenters, and at different maximum loads P_{max}.

The cone cracks in the glass layers were observed *in situ* during loading using a video camera system, chiefly from the side but sometimes from below.[20,23] Such observations enabled the entire crack evolution to be followed from inception to failure. Depth c of outer and inner cracks was thereby measured as a function of number of cycles n (or test duration t) for each test condition. In each case the cracks were measured at their deepest point; in the case of inner cones, this sometimes meant switching from one segment of the penetrating cone to another. In some cases the test was stopped after a certain number of cycles and the specimen

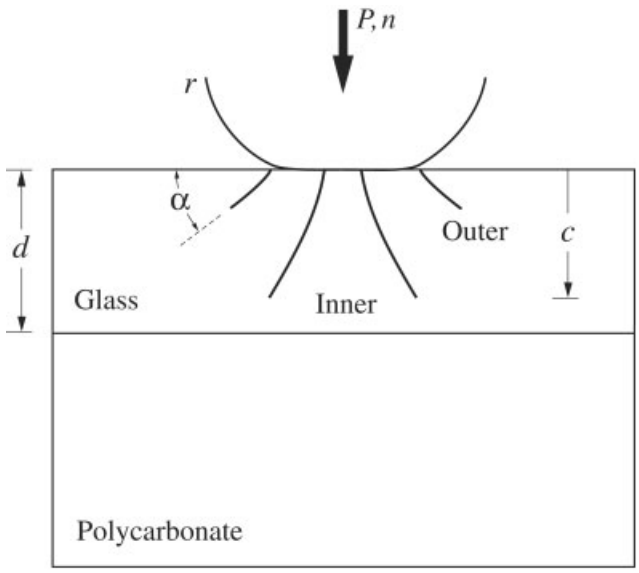

Figure 2. Schematic of crack geometry for cyclic contact with sphere of radius r at load P and number of cycles n on glass layer of thickness d on polycarbonate substrate, showing outer- and inner-cone cracks of depth c and angle α.

examined in transmitted light, specifically to determine the incidence of any top-surface radial cracking.[17]

RESULTS AND ANALYSIS

Outer- and Inner-Cone Crack Morphology

This subsection describes basic elements of outer- and inner-cone crack morphology in glass monoliths and glass/polycarbonate bilayers. Under the test conditions used here, that is, $P_{max} = 120$ N and $P_{min} = 2$ N at 1 Hz in water, and etched undersurfaces, cone cracks remained the dominant mode of fracture.

Figure 3 shows a typical sequence of events in a glass monolith specimen. Both cone types grow predominantly during the loading half-cycles. After a few cycles an outer cone initiates [Figure 3(a)] and propagates downward and outward [Figure 3(b)] in classical fashion.[16] Subsequently, an inner cone appears below the outer-cone base [Figure 3(c)] and extends downward at a relatively high rate [Figure 3(d,e)]. The inner cone appears as individual finger-like segments, some of which may begin slowly but may ultimately overtake their predecessors [Figure 3(f)], reflecting some axial asymmetry and irregularity in the crack front. Intrusion of water into the crack interface reduces visibility of the inner cones. After extended cycling to $n \approx 10^6$ cycles (not shown), the cracks tended to stabilize. Top-surface inspection after cycling confirmed outer- and inner-cone crack traces of the type seen in Figure 1.[17] Measurements of crack angles in several specimens yielded $\alpha = 23 \pm 5°$ for outer cones,[11,24] and $\alpha = 55 \pm 15°$ for inner cones.

A comparable sequence for glass/polycarbonate bilayers under near-identical test conditions is shown in Figure 4. The main difference between the bilayer and monolith sequences is a slight reduction in cone crack depths in the early stages of loading [Figure 4(a,b)], but substantial increases in depths in the intermediate [Figure 4(c,d)] and later stages [Figure 4(e,f)]. Notable in this sequence is the appearance of a water-filled kidney-shaped crack segment extending rapidly downward [Figure 4(e)], followed by abrupt penetration of the inner cone to the bilayer interface [Figure 4(f)]. Interestingly, no clear indication of any coating/substrate interfacial delamination of the kind envisioned by others[19] was observed here, even after continuation of loading to $n \approx 10^6$ cycles (not shown), attesting to the good bonding between glass and polycarbonate. Crack angles were not significantly different from those in the glass monoliths.

An effort was made to check for other damage modes, most notably radial cracking, by looking from below the specimens during testing and in transmitted light at various stages of test interruption. Such cracks were indeed observed in the near-contact zone after extensive cycling,[17] but not until well after substantial growth of the inner cones, somewhere after stage (d) or (e) in Figures 3 and 4.

Crack-Size Measurements

In this section the differences between outer- and inner-cone crack evolution is quantified by measuring crack depths c as a function of number of cycles n or test duration t. As noted in Figure 3, some cracks (especially the inner cones) grew asymmetrically, so that occasionally one crack segment overtook a predecessor. Accordingly, in all quantitative tests, each crack depth was measured at the point of maximum penetration for prescribed values of n in the video sequences. Again, the tests in this subsection were carried out at $P_{max} = 120$ N and $P_{min} = 2$ N at 1 Hz in water.

Figure 5 compares outer- and inner-cone crack evolution in (a) monolithic glass and (b) glass/polycarbonate bilayers, as penetration depth $c(n)$. Data points are individual measurements, for three cracks in each specimen type. Unfilled symbols indicate outer cones, filled symbols inner cones. Arrows indicate instabilities in the crack growth. The trends in Figure 5 reflect those observed in Figures 3 and 4. In the monolith specimens, the outer cones initiate between $n = 1$–10 cycles and propagate rapidly to a depth $c \approx 100$ μm before leveling out over the remaining data range. The inner cones initiate considerably later, at $n \approx 10^3$ cycles, but soon overtake their outer counterparts and propagate substantially deeper, to $c \approx 500$ μm, over the same data range. In the bilayers, initiation conditions remain somewhat similar to those in the monoliths. However, the outer cones pop into a slightly shallower depth. More importantly, the inner cones quickly grow much deeper, becoming more unstable as they begin to experience flexural tensile stresses, ultimately penetrating abruptly to the glass/polycarbonate interface.

Figure 6 compares crack evolution data for cyclic testing at (a) $f = 10$ Hz and (b) $f = 1$ Hz, as well as in (c) static

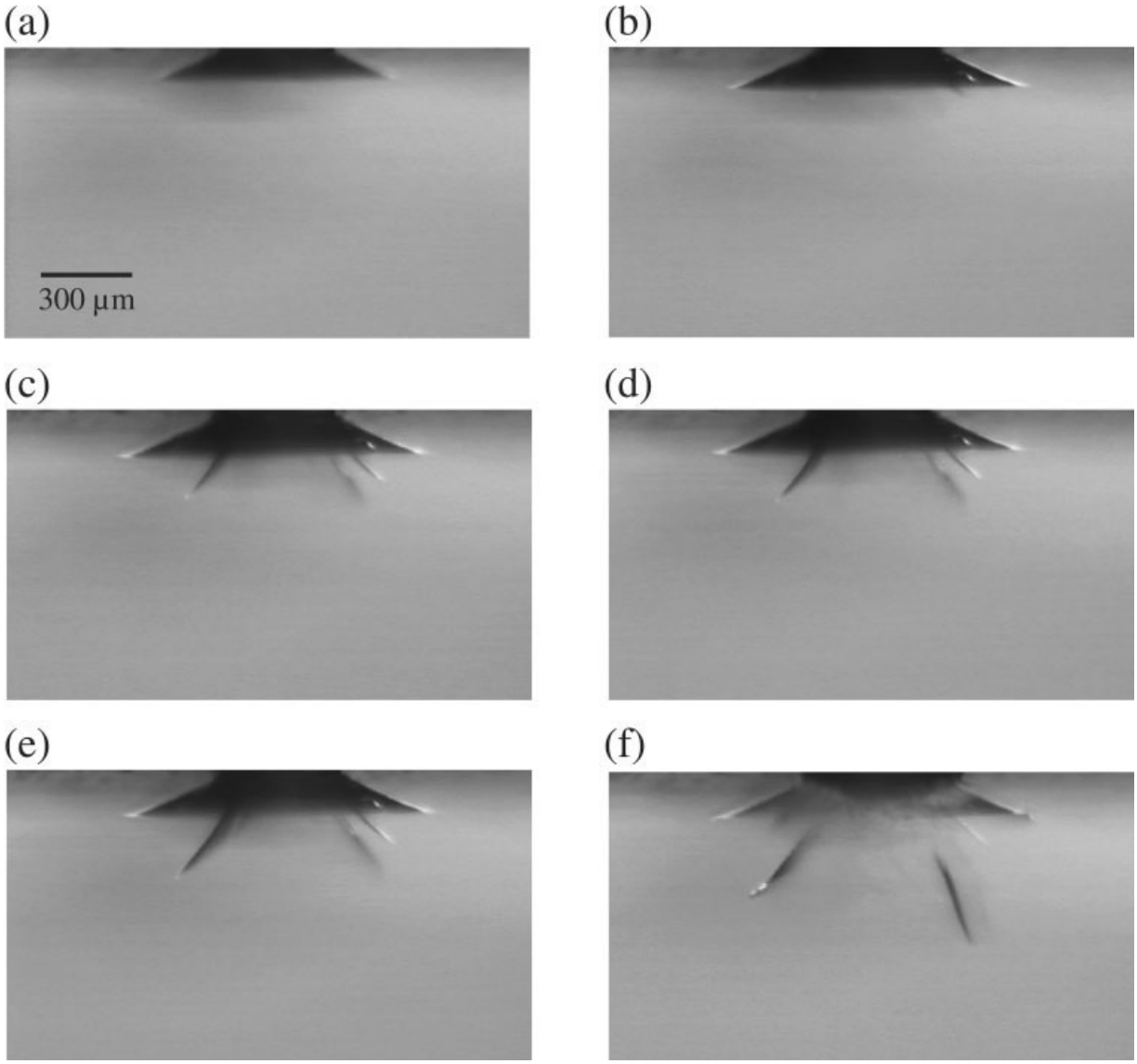

Figure 3. Video side views of cone crack evolution in soda-lime glass monolith (top surface abraded), indentation with WC sphere of radius $r = 1.59$ mm, cyclic loading between $P_{max} = 120$ N and $P_{min} = 2$ N at 1 Hz, in water: (a) $n = 6$ cycles, (b) $n = 1.1 \times 10^3$ cycles, (c) $n = 7.0 \times 10^3$, (d) $n = 1.0 \times 10^4$, (e) $n = 2.5 \times 10^4$, (f) $n = 1.6 \times 10^5$. Note steady growth of inner-cone crack segments.

loading at a common maximum load. To facilitate intercomparison, the data in this figure are plotted as a function of test duration t ($= n/f$ for cyclic tests) rather than of n. Again, unfilled symbols indicate outer cones and filled symbols inner cones, with arrows indicating instabilities. The data for outer cones show a similar trend in all cases, suggesting a common time-dependent slow crack growth mechanism. However, the data for the inner cones show substantial shifts between the 10-Hz and 1-Hz data, consistent with a mechanical fatigue mechanism dependent only on number of cycles. Note the absence of any data at all for inner cracks in static loading in Figure 6(c), confirming a dominant mechanical driving force for this crack system.

Basic fracture mechanics analysis may be used to quantify the data trends in Figures 5 and 6. For cone cracks extending by slow crack growth in Hertzian contact fields, cyclic or static, analysis gives $c \propto (n/f)^{2/3N} \propto t^{2/3N}$, where N is a crack velocity exponent.[17] This dependence is included as the inclined lines in Figures 5 and 6, with common slope (corresponding to $N = 17$ for soda-lime glass)[17] and intercept, and signifies a pronounced slowdown with extension as the crack propagates away from the contact force. Whereas the well-developed outer cones follow this classical slow crack growth dependence to reasonable approximation, the inner cones follow a much steeper curve, closer to a linear relation $c \propto t$, indicating a sustained driving force throughout the entire crack evolution.

Additional Tests

Additional cyclic tests at $f = 1$ Hz were made on the glass/polycarbonate bilayers to investigate the influence of extra-

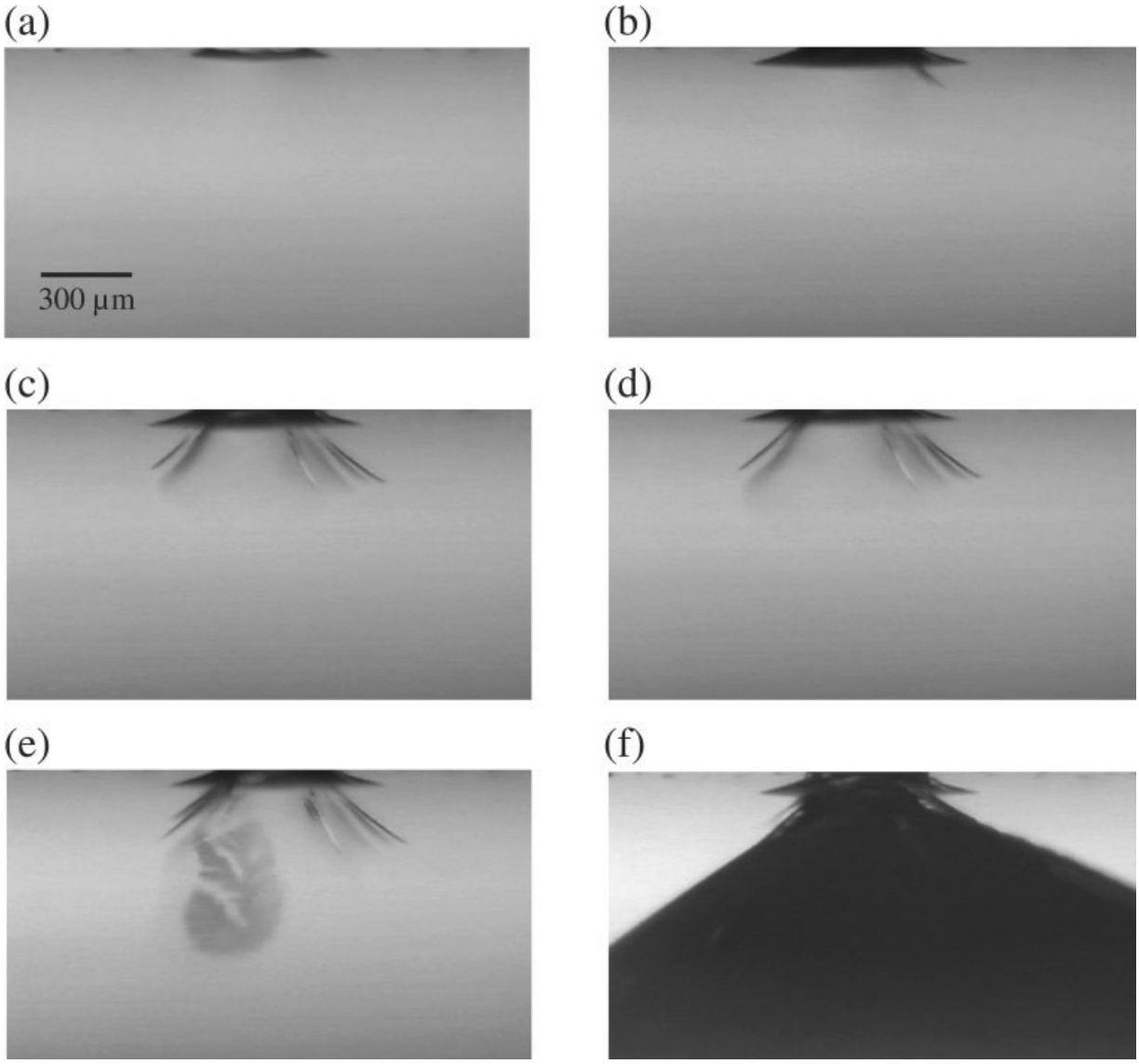

Figure 4. Video side views of cone crack evolution in soda-lime glass of thickness $d = 1$ mm (top surface abraded) on polycarbonate substrate, indentation with WC sphere of radius $r = 1.59$ mm, cyclic loading between $P_{max} = 120$ N and $P_{min} = 2$ N at 1 Hz, in water: (a) $n = 6$ cycles, (b) $n = 2.1 \times 10^3$, (c) $n = 7.0 \times 10^3$, (d) $n = 1.0 \times 10^4$, (e) $n = 2.5 \times 10^4$, (f) $n = 2.5 \times 10^4$. Note accelerated growth of inner-cone crack segments in (e) and (f).

neous variables—surface flaw state, indenter/specimen elastic mismatch, and environment—under testing conditions otherwise similar to those in Figures 3–6. Tests on acid-etched relative to abraded top surfaces indicated a higher number of cycles to initiate outer cones, as expected for surfaces with smaller and more sparse flaws. However, once the outer cones formed and entered the contact far field, they reached depths similar to those in the abraded specimens, again as expected. Most interestingly, the flaw state made little discernible difference to the evolution of inner cones, either initiation and propagation. This suggests that the flaw state in the annular contact fretting region of Figure 1, where the inner cones form, may be governed by extraneous damage from asperities on the indenting sphere.[17]

Effects of elastic mismatch were investigated using glass instead of WC spheres, of the same radius r. Again, it took a higher number of cycles to initiate outer cones, partly because of reduced stress intensity beneath the softer indenter and possibly also because of reduction of frictional tractions at the indenter/specimen interface.[18] However, inner cones still formed, and at similar critical number of cycles (within data scatter bounds), as for WC indenters. This last result would appear to eliminate elastic mismatch as a primary cause of inner-cone crack development.

Finally, some cyclic tests were conducted in air instead of water to ascertain the influence of environment. Outer-cone cracks initiated much more slowly in air than in water (by a factor of 10^2–10^3 in n), consistent with a slower crack veloc-

ity in the gaseous environment.[25,26] Tellingly, no inner-cone cracks were observed at the operating load P_{max} = 120 N up to 10^6 cycles, or in tests at loads up to P_{max} = 500 N over the same cycle range, indicating that liquid environment is an essential requirement for formation of this crack type.

DISCUSSION

This study has examined fracture modes in glass/polycarbonate bilayers in cyclic loading with spherical indenters in water, in simulation of crown/tooth occlusal contact in dental function. Abraded soda-lime glass was selected as the model brittle material, representative of porcelain materials used in dental crowns[17] (and indeed to some extent of natural enamel[27,28]). Abrading the glass top surface reduces the strength to that of porcelain, by introducing flaws comparable in scale to those associated with crystallites in the porcelain interior. Glass has the distinct advantage of transparency, enabling *in situ* viewing of crack evolution through the entire loading process. For the glass thickness of 1 mm used here, the dominant stress state is that of Hertzian contact. The corresponding principal mode of fracture is top-surface cone cracking.[9] Classical outer-cone cracks grow steadily in either static or cyclic loading, in accordance with a slow crack growth mechanism associated with the influence of water molecules.[12,13,17,29] Inner-cone cracks, relatively unexplored

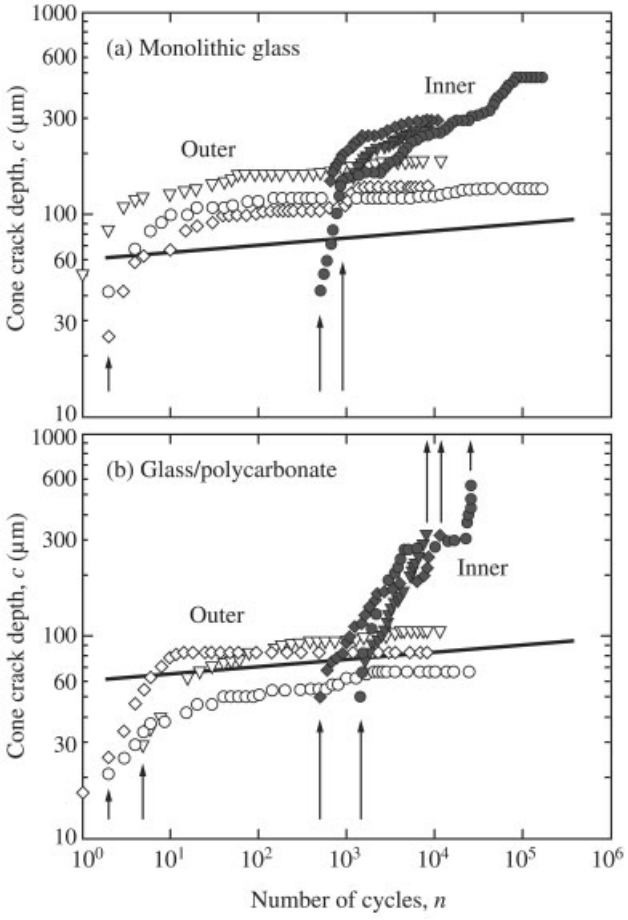

Figure 5. Crack depth c as function of number of cycles n for cone cracks in top-surface-abraded glass. (a) Monolithic plate and (b) 1-mm plates bonded to polycarbonate base. Tests at P_{max} = 120 N and P_{min} = 2 N, frequency 1 Hz, in water. Vertical arrows indicate regions of crack instability. Inclined solid lines indicate expected response from slow crack growth.

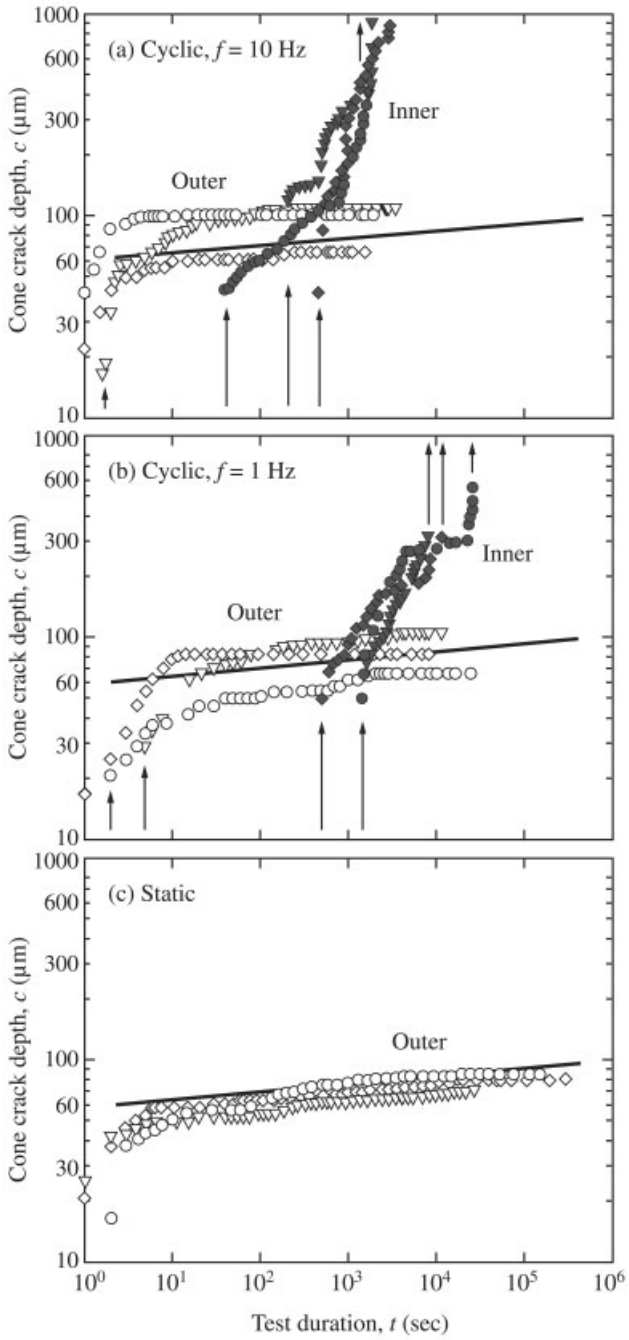

Figure 6. Crack depth c as function of test duration t for cone cracks in top-surface-abraded 1-mm glass plates bonded to polycarbonate bases. Cyclic tests at (a) 10 Hz and (b) 1 Hz, and (c) static tests, for P_{max} = 120 N, in water. Vertical arrows indicate regions of crack instability. Inclined solid lines indicate expected response from slow crack growth. Note absence of inner cone in static loading.

until now, appear predominantly in cyclic loading in water. These inner cracks grow in bilayers much as in monoliths, more slowly initially, but subsequently more quickly, owing to a superposed (albeit secondary) flexural stress field. It is the tendency for inner cones to accelerate toward the lower interface in their later stages [Figures 4(f) and 5] that renders the bilayer structure especially vulnerable. Although the incidence of cone cracks may not degrade the tensile strength of ceramic components as severely as other modes (e.g., radial cracks),[17] they may nevertheless provide pathways for external elements to the interior of the layer system—and, in the case of weak interfaces, become a source of interlayer delamination.[19]

The question then arises at to the source of the mechanical forces that drive the inner-cone cracks. These cracks appear to initiate close to the inner boundary of a fretting annulus within the greater contact circle (Figure 1). Three contributing factors may be considered:

1. Indenter/specimen elastic mismatch. If the indenter and immediate specimen materials have different elastic moduli, frictional slip can occur in an outer annulus at the contact interface.[18,30] Such slip can impose additional radial contact stresses, which reverse during loading/unloading, enhancing local tension within the contact zone. However, although frictional slip may exacerbate surface fretting, especially in the case of WC indenters (where elastic mismatch relative to glass is high), it cannot be the principal cause, because inner cones form almost as readily using glass indenters (where the mismatch is zero).
2. Cumulative quasiplasticity. Another potential mechanism is buildup of residual stresses from cumulative quasiplasticity below the immediate contact surface, particularly in the vicinity of the fretting zone. In monolithic ceramics, the source of radial cracks is residual tensile stress at the quasiplastic zone boundary. Quasiplasticity is a result of microstructural breakdown from local shear stresses below the contact, leading to intensive damage accumulation.[8,16,31–33] Although it is most evident in softer, more heterogeneous ceramics, quasiplasticity can become a factor in the most brittle of materials, including glass and porcelain.[17,33] The depth of any quasiplastic zone increases steadily downward from the fretting zone with continued cycling.[34] This mode is augmented by the entry of water into weakened shear fault interfaces.[33,35] Although the presence of starting flaws (e.g., from abrasion) may provide starting sites for quasiplasticity, shear faults may initiate at initially defect-free (e.g., etched) surfaces from generation of local stress concentrations (e.g., from microcontacts with indenter asperities). However, because the quasiplasticity zones are generally confined to a volume immediately below the contact area, this mode of deformation would appear incapable of explaining the persistent long-range propagation of the inner cones into the deep sublayer.
3. Hydraulic pumping. Another potential source of mechanical driving force is hydraulic pumping as confined water ingresses and egresses the crack interface under pressure during the loading and unloading half-cycles. That water does enter the crack is indisputable—recall the mottled appearance of the water-filled kidney-shaped crack segment in Figure 4(e). Hydraulic pressure has long been considered a primary mode of fatigue-crack initiation and propagation in lubricated rolling contact configurations.[21,36,37] Water intrusion can force open surface flaws or fissures in the immediate contact zone, and can drive cracks deep into the sublayer by forcing entrapped liquid toward the crack tip. Continual extension allows more water to enter the crack interfaces in subsequent cycles, thereby generating an ever-persistent long-range driving force, even as the cracks penetrate deep into the sublayer. That such a mechanism can exert the necessary forces needed to drive the inner cones through an entire plate (Figures 4–6) is evidenced by the occasional failure of very thick (3 mm) monolithic specimens during cycling in water at high contact loads.[17,33]

In view of the potentially destructive nature of the inner-cone cracks, more definitive experiments to elucidate the intrinsic mechanisms of the fracture evolution and to develop appropriate fracture mechanics descriptions appear to be warranted.

Although clearly deleterious, inner-cone cracks are still less dangerous than their main competitor—radial cracks. As already indicated, radial cracks are readily generated from quasiplastic zones in softer, coarser polycrystalline ceramics and in contacts with sharper indenters.[38] They are observed in the present experiments, again especially in water, although in this case only after development of the inner cones. Once they do form, quasiplastically induced radial cracks provide a potent source of failure, because they are oriented normally to any ensuing flexural tensile stresses. Similar radial cracks can also occur at the bottom surface of brittle plates on compliant supporting substrates, but in that case from naturally occurring flaws. Those latter radial cracks become dominant as the plate thickness is diminished much below 1 mm, that is, as the stress concentrations shift from the top to the bottom surface, and in plates with severe undersurface abrasion preparation.[39]

In the specific context of dental crowns, it is clear that any sound design strategy requires due attention to the various failure modes. The first requirement is to maintain an adequate crown thickness, in order to avoid bottom-surface radials at all costs. Fatigue of the porcelain veneer from continued growth of inner-cone cracks could become a problem in such crowns, particularly in cases where the opposing cuspal radii are relatively small, leading to uncommonly high local stress concentrations.[38] The presence of oral fluids and the superposition of complex loading cycles (including tangential and rotational components) can only make matters worse. Penetration of inner-cone cracks to the dentin subsurface offers pathways to infection, if not total failure of the crown. The presence of stiff and strong ceramic-core layers may offer some protection by arresting any such penetrating

cracks, but then the system may become susceptible to delamination of the veneer. Additional effects of any residual stresses in the veneer from thermal expansion mismatch relative to the core could be an additional factor.

The same manner of contact loading pertains to force states in ceramic acetabular liners (typically 4–5 mm thick) with polyethylene backing in total hip replacements, although there the nature of the contact is considerably more complex.[4,5]

Discussions with Herzl Chai, Yeon-Gil Jung, Yan Deng, E. Dianne Rekow, Van P. Thompson, and Hee-Soo Lee are gratefully acknowledged.

REFERENCES

1. Lawn BR. Ceramic-based layer structures for biomechanical applications. Curr Opinion Solid State Mater Sci 2002;6:229–235.
2. Lawn BR, Pajares A, Zhang Y, Deng Y, Polack M, Lloyd IK, Rekow ED, Thompson VP. Materials design in the performance of all-ceramic crowns. Biomaterials 2004;25:2885–2892.
3. Lawn BR, Pajares A, Miranda P, Deng Y. In: Encyclopedia of Materials: Science and Technology. Oxford: Elsevier; in press. p 3286–3290.
4. Willmann G. Ceramic femoral heads for total hip arthroplasty. Adv Eng Mater 2000;2:114–122.
5. Willmann G. Improving bearing surfaces of artificial joints. Adv Eng Mater 2001;3:135–141.
6. Jung YG, Wuttiphan S, Peterson IM, Lawn BR. Damage modes in dental layer structures. J Dent Res 1999;78:887–897.
7. Lawn BR, Lee KS, Chai H, Pajares A, Kim DK, Wuttiphan S, Peterson IM, Hu X. Damage-resistant brittle coatings. Adv Eng Mater 2000;2:745–748.
8. Lawn BR, Deng Y, Miranda P, Pajares A, Chai H, Kim DK. Overview: damage in brittle layer structures from concentrated loads. J Mater Res 2002;17:3019–3036.
9. Deng Y, Lawn BR, Lloyd IK. Characterization of damage modes in dental ceramic bilayer structures. J Biomed Mater Res 2002;63B:137–145.
10. Shrotriya P, Wang R, Katsube N, Seghi R, Soboyejo WO. Contact damage in model dental multilayers: an investigation of the influence of indenter size. J Mater Sci Mater Med 2003;14:1726.
11. Frank FC, Lawn BR. On the theory of Hertzian fracture. Proc R Soc London Ser A 1967;299:291–306.
12. Langitan FB, Lawn BR. Effect of a reactive environment on the Hertzian strength of brittle solids. J Appl Phys 1970;41:3357–3365.
13. Mikosza AG, Lawn BR. Section-and-etch study of Hertzian fracture mechanics. J Appl Phys 1971;42:5540–5545.
14. Wilshaw TR. The Hertzian fracture test. J Phys D Appl Phys 1971;4:1567–1581.
15. Lawn BR, Wilshaw TR. Indentation fracture: Principles and applications. J Mater Sci 1975;10:1049–1081.
16. Lawn BR. Indentation of ceramics with spheres: A century after Hertz. J Am Ceram Soc 1998;81:1977–1994.
17. Kim DK, Jung YG, Peterson IM, Lawn BR. Cyclic fatigue of intrinsically brittle ceramics in contact with spheres. Acta Mater 1999;47:4711–4725.
18. Johnson KL, O'Connor JJ, Woodward AC. The effect of indenter elasticity on the Hertzian fracture of brittle materials. Proc R Soc London Ser A 1973;334:95.
19. Davis JB, Cao HC, Bao G, Evans AG. The fracture energy of interfaces: An elastic indentation technique. Acta Metall 1991;39:1019–1024.
20. Chai H, Lawn BR, Wuttiphan S. Fracture modes in brittle coatings with large interlayer modulus mismatch. J Mater Res 1999;14:3805–3817.
21. Hanson MT, Keer LM. An analytical life prediction model for the crack propagation occurring in contact fatigue failure. Tribol Trans 1992;35:451–461.
22. Lawn BR, Deng Y, Thompson VP. Use of contact testing in the characterization and design of all-ceramic crown-like layer structures: a review. J Prosthet Dent 2001;86:495–510.
23. Deng Y, Miranda P, Pajares A, Lawn BR. Fracture of ceramic/ceramic/polymer trilayers for biomechanical applications. J Biomed Mater Res 2003;67A:828–833.
24. Kocer C, Collins RE. The angle of Hertzian cone cracks. J Am Ceram Soc 1998;81:1736–1742.
25. Wiederhorn SM, Bolz LH. Stress corrosion and static fatigue of glass. J Am Ceram Soc 1970;53:543–548.
26. Wiederhorn SM. A chemical interpretation of static fatigue. J Am Ceram Soc 1972;55:81–85.
27. Xu HHK, Smith DT, Jahanmir S, Romberg E, Kelly JR, Thompson VP. Indentation damage and mechanical properties of human enamel and dentin. J Dent Res 1998;77:472–480.
28. Cuy JL, Mann AB, Livi KJ, Teaford MF, Weihs TP. Nanoindentation mapping of the mechanical properties of human molar tooth enamel. Arch Oral Biol 2002;7:281–291.
29. Lawn BR, Jakus K, Gonzalez AC. Sharp vs blunt crack hypotheses in the strength of glass: a critical study using indentation flaws. J Am Ceram Soc 1985;68:25–34.
30. Kennedy PJ, Conte AA, Whitenton EP, Ives LK, Peterson MB. In: S. Jahanmir, editors. Friction and wear of ceramics. New York: Marcel Dekker; 1994. p 79–98.
31. Lawn BR, Padture NP, Cai H, Guiberteau F. Making ceramics "ductile." Science 1994;263:1114–1116.
32. Padture NP, Lawn BR. Contact fatigue of a silicon carbide with a heterogeneous grain structure. J Am Ceram Soc 1995;78:1431–1438.
33. Jung YG, Peterson IM, Kim DK, Lawn BR. Lifetime-limiting strength degradation from contact fatigue in dental ceramics. J Dent Res 2000;79:722–731.
34. Lawn BR, Kim DK, Lee SK, Jung YG, Peterson IM. In: Wu XR, Wang ZG, editors. The Seventh International Fatigue Conference, Fatigue 99. Beijing: Higher Education Press; 1999. Vol. 1, p 69–80.
35. Lawn BR, Dabbs TP, Fairbanks CJ. Kinetics of shear-activated indentation crack initiation in soda-lime glass. J Mater Sci 1983;18:2785–2797.
36. Kaneta M, Yatsuzuka H, Murakami Y. Mechanism of surface crack growth in lubricated rolling/sliding spherical contact. ASLE Trans 1985;8:407–414.
37. Bower AF. The influence of crack face friction and trapped fluid on surface initiated rolling contact fatigue cracks. J Tribol 1988;110:704–711.
38. Rhee YW, Kim HW, Deng Y, Lawn BR. Brittle Fracture Versus Quasiplasticity In Ceramics: A Simple Predictive Index. J Am Ceram Soc 2001;84:561–565.
39. Rhee YW, Kim HW, Deng Y, Lawn BR. Contact-induced damage in ceramic coatings on compliant substrates: Fracture mechanics and design. J Am Ceram Soc 2001;84:1066–1072.